Numerical investigations on axial and radial blade rubs in turbo-machinery

Numerical investigations on axial and radial blade rubs in turbo-machinery

You may also be interested in:

Flow performance of highly loaded axial fan with bowed rotor blades
L Chen, X J Liu, A L Yang et al.

Influence of the conservative rotor loads on the near wake of a wind turbinex
I. Herráez, D. Micallef and G.A.M. van Kuik

Helicopter measures air density
Andy Ellison

Inspection of Rotor and Stator Vibration of the Ultrasonic Motor Using Longitudinal and Torsional Vibrations
Manabu Aoyagi and Yoshiro Tomikawa

Trial Construction of a Noncontact Ultrasonic Motor with an Ultrasonically Levitated Rotor
Tohgo Yamazaki, Junhui Hu, Kentaro Nakamura et al.

Experimental and numerical investigations on adhesively bonded joints
R Negru, L Marsavina and M Hluscu

Revolution Speed Characteristics of an Ultrasonic Motor Estimated from the Pressure Distribution of the Rotor
Hiroshi Hirata and Sadayuki Ueha

Computational Fluid Dynamics based Fault Simulations of a Vertical Axis Wind Turbines
Kyoo-seon Park, Taimoor Asim and Rakesh Mishra

Resonant Mode Design for Noncontact Ultrasonic Motor with Levitated Rotor
Junichi Saito, James Robert Friend, Kentaro Nakamura et al.

Numerical investigations on axial and radial blade rubs in turbo-machinery

Ahmed M Abdelrhman[1], Eric Sang Sung Tang[1], M Salman Leong[2], Haidar F Al-Qrimli[3], G Rajamohan[1].

[1]Curtin University Malaysia, CDT 250 98009, Miri, Sarawak, Malaysia
[2]Institute of Noise and Vibration, University Technology Malaysia, Malaysia
[3]Heriot-Watt University, 62200 Putrajaya, Malaysia

Email: ahmed.mohammed@curtin.edu.my

Abstract. In the recent years, the clearance between the rotor blades and stator/casing had been getting smaller and smaller prior improving the aerodynamic efficiency of the turbomachines as demand in the engineering field. Due to the clearance reduction between the blade tip and the rotor casing and between rotor blades and stator blades, axial and radial blade rubbing could be occurred, especially at high speed resulting into complex nonlinear vibrations. The primary aim of this study is to address the blade axial rubbing phenomenon using numerical analysis of rotor system. A comparison between rubbing caused impacts of axial and radial blade rubbing and rubbing forces are also aims of this study. Tow rotor models (rotor-stator and rotor casing models) has been designed and sketched using SOILDSWORKS software. ANSYS software has been used for the simulation and the numerical analysis. The rubbing conditions were simulated at speed range of 1000rpm, 1500rpm and 2000rpm. Analysis results for axial blade rubbing showed the appearance of blade passing frequency and its multiple frequencies (1x, 2x 3x etc.) and these frequencies will more excited with increasing the rotational speed. Also, it has been observed that when the rotating speed increased, the rubbing force and the harmonics frequencies in x, y and z-direction become higher and severe. The comparison study showed that axial blade rub is more dangerous and would generate a higher vibration impacts and higher blade rubbing force than radial blade rub.

1. Introduction

In order to improve performance and aerodynamics efficiency of the turbomachines, the clearance between the rotor and stator and between the rotor and the casing has to be minimized to become smaller. Due to the smaller clearance, the occurrence of blade rubs when the rotor is contacted with stator or the casing at a certain operating speed and that will probably result in high nonlinear vibration and finally could lead to severe machine damage. Blade rubbing is known to be a very serious malfunction in turbomachinery and it's reported to be 42% from the total malfunctions in rotating machinery [1, 2]. The clearance between the rotating blades and the inner surface of the rotor casing and the stator blades has to be designed to be as smaller for better efficiency. However, this will obviously lead to blade rubbing and also the excessive vibration which could lead to the failures of blades in turbine engines. The complicated vibration generated due to the rubbing also could cause a reduction of performance in the system and shorten lives of the blades. The occurrence of the rub-impact could also lead to the high vibrational level, high temperature, light wearing rate and finally could result in blade loss. The

instantaneous huge unbalance that caused by the blade loss could also lead to severe blade rubs. Therefore, the rubbing is frequently occurred in the turbine engines during the operation due to the centrifugal effects.

As reported by Zhang and Chen. [3], many researchers investigated the rotor-stator interactions using different methods such as an analytical, numerical and experimental method. For example, Zhang and Chen. [3], studied on the jump phenomena and full annular rub of Jeffcott rotor by analytical and numerical methods. They also tended to investigate the feature of the rotor response which will be affected by rotational speed and the system rotor parameter based on Routh-Hurwitz criteria. Lu and Chu. [4], proposed an improved model of a vertical Jeffcott rotor with the polar equation in order to investigate the nonlinear dynamics characteristics on radial and torsional vibration of a rotor under full annular rub, partial rub and no-rub conditions. Tai, Ma, Liu, Liu and Wen. [5], presented a lumped mass model of a single rub-impact rotor system for analysing the nonlinear steady-state response of the system depended on the size of the gap, the stiffness of stator and unbalance. Choy and Padovan. [6], investigated the characteristics of the non-linear dynamics of rubbing between rotor and casing and also the relevance of the variety of rubbing excitation parameters such as rub force and energy levels to rubbing duration and incidence separation angles. In order to understand the mechanisms of blade rubbing, Laverty. [7], studied the mechanics of rubbing between compressor blade tip seals and rotor casing. They found that the incursion rate of the rubbing is mainly contributed to the overall rubbing energy. Cao, Yang, Chen, Wang, Jiang, Li, Wei and Zhao. [8] suggested a hysteretic contact force model (HCFM) under hard coating and soft coating of the equations Yuan, Chu and Hao. [9], employed an unbalance and axial rub-impact rotor model with the derivation of Lagrangian equation to all six degrees of freedom and the ODE solvers in Matlab for numerical simulation. Zhang and Ding. [10], conducted a numerical calculation on the lateral and torsional vibration of a rotor system with axial-rub between disk and stator based on the lateral coupled equations, the torsional motion of the rotor and lateral motion of disk. Ma, Yin, Tai, Wang and Wen. [11], investigated the dynamic behavior between rotating blade and casing under rubbing condition with a constant rotational speed at the run-up process. They were noticed that the steady process was occurred at 10000rpm by considering the effects of the static misalignment, stiffness of casing, deformation of the casing and the vibration response due to the intermittent rubs. Ma, Yin, Wu, Tai and Wen. [12], simulated a bladed rotor system with blade tip rubbing. They observed the appearance of the blade passing frequency (BPF) and its multiple frequencies are shown very obvious when four blades were rubbing with the rotor casing compared to single blade rubbing condition. The current author also investigated experimentally the blade radial rub-impact in multi-stage rotor system [13-15].

The investigations on the axial dynamic behaviour of axial rub-impact seem to be relatively few. This study is intended to investigate the axial dynamic behaviour of axial rub-impact a rotor system with a single stage at different operating speeds via numerical simulation using ANSYS software. Consequently, a comparison between the axial rub-impact and radial rub-impact is also discussed in this study.

2. Simulation procedures

2.1. Models design specifications:
To study the effects of blade axial rubbing impact, vibration phenomena and the rubbing force, two rotor models (rotor-stator model and rotor casing model) were designed using 3D modeling software (SolidWorks), see figure (1). The blading system is identical in both models. For rotor-stator model, the rotor blade is designed based on the geometric properties while the stator blade is designed as the same geometric properties of a rotor blade with the additional width of 9mm and thickness of 10mm. The penetration depth of the rotor blade and stator blade and between the rotor blades tip and rotor inner casing is 6mm. The geometric properties of the rotor blade, stator blade, and rotor casing are tabulated in Table 1).
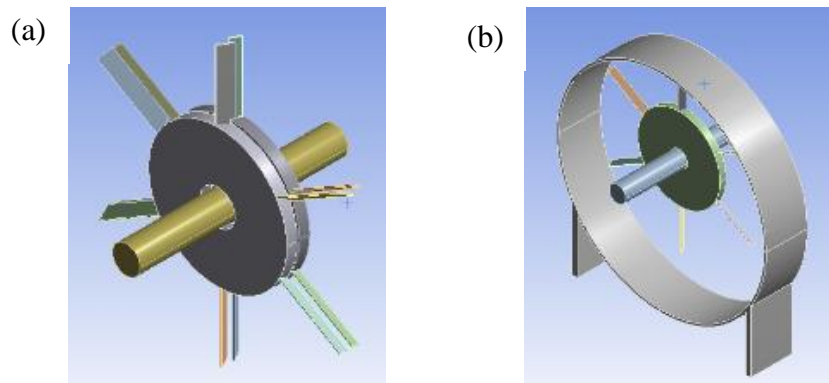
Figure 1. (a) Rotor-Stator Model, (b) Rotor-Casing Model

Table 1. Material and Geometric Parameters

Part	Material Parameter	Geometric Parameter
Shaft	Density: 7850 kg/m^3, Shear modulus: 75GPa	Length: 0.6m, Radius: 0.04m
Disk	Density: 7850 kg/m^3, Young's modulus: 200GPa, Poisson's ratio: 0.3	Radius: 0.2m, Thickness: 0.03m
Blade, n=6	Density: 7850 kg/m^3. Young's modulus: 200GPa	Length: 0.2m, Width: 0.03m, Thickness: 0.004m, Stagger angle, θ: 30^0
Casing	Density: 7850 kg/m^3, Young's modulus: 200GPa, Poisson's ratio: 0.3	Inner Radius: 0.5m, Outer Radius: 0.51m, Length: 0.2m, Length of support: 0.3m

2.2. Meshing Independence

Meshing is an important part in any computer simulation. Meshing is creating of some grid-points "nodes" connected to another nodes "element". In order to acquire good solution results, the more number of elements or nodes created the higher accuracy of the solution could be achieved in ANSYS. In this study, meshing independence is applied by altering the element sizes for the validation with Yang's model by comparing the lowest absolute error between the present model and Yang's model. Therefore, 0.3m, 0.002m and 0.006m of element sizes are adopted, as shown in Figure 2.
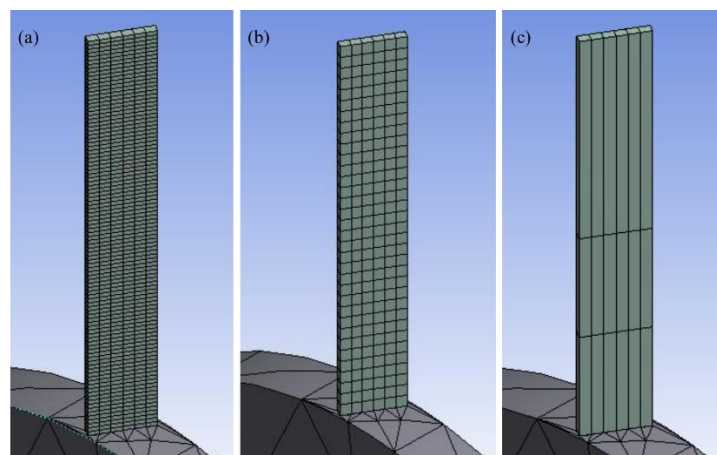

Figure 2, (a) Blade with Element Size of 0.002m, (b) Blade with Element Size of 0.006m, (c) Blade with Element Size of 0.3m

2.3. Boundary Condition

In the analysis of rotor-stator model by ANSYS, the stationary part (stator) was set to be fixed at all the directions which the translation in X, Y and Z directions were arrested in order to prevent the rotation in all degrees of freedom. A rotational speed of 1000rpm, 1500rpm and 2000rpm was applied respectively on the z-axis of the shaft of the rotor system. The occurrence of the axial rubbing between the rotor blade and stator blade is occurring when the rotor starts rotating. Meanwhile, for the rotor-casing model, the frictional coefficient is assumed as 0.246 and a rotational speed of 1000rpm was applied on the z-axis of the shaft. The occurrence of the radial rubbing between the blade tips and the rotor inner casing is simulated and investigated and its impacts will be compared with blade axial rub impacts. The total simulation time id set to be 1.2 second, the run-up process starts from t = 0 to 0.2s and run-down process start from t= 1s to 1.2s while the constant rotational speed is from t = 0.2s to t = 1s.

2.4. Contact analysis

The contact region has to establish the relationship between the surfaces of the two contacted objects in order to avoid them just passing through each other without any effect. In this study, both models are simulated using transient structural analysis in ANSYS 15 Workbench. The type of contact applied between the rotor blade and stator blade is frictionless contact while the contact between the blade tip and the inner casing is frictional contact type. The frictionless contact is applied for the rotor-stator model as the contact between the rotor blade and stator blade is far open with the penetration depth. Meanwhile, the frictional contact is applied for the rotor-casing model as the contact between the inner casing and the tip of the rotor blade is closed with penetration depth.

2.5. Unstressed Modal and Pre-stressed Modal Analysis

Modal Analysis was conducted in ANSYS Workbench 15.0 for both unstressed and pre-stressed models. For unstressed modal analysis, the stress does not taken into account for the analysis while for the pre-stressed modal analysis, there is the stress initialization due to the centrifugal force during the rotation of the rotor blade. A constant centrifugal force will be experienced by an object when it is rotating with a constant angular velocity given by equation:

$$F = m\omega^2 r \tag{1}$$

where F is the centrifugal force, m is the mass of the spinning object, ω is the angular velocity and r is the radial distance from the axis of rotation. In this study, the rotational speed of the rotor is set to be 1000rpm and 1500rpm and 2000rpm respectively. It is believed that the frequency response of the system can be altered by the stress stiffening where the natural frequencies changed with the speed of the rotor. Presence of unexpected resonances is expected when the natural frequencies changed with the high speed of the rotor system.

Table 2. Unstressed Modal Analysis

Mode	Stator	Vibrational Mode	Rotor	Vibrational Mode
		Unstressed Modal Analysis		
1	78.016	First Flap-wise (blade)	81.065	First Flap-wise (blade)
2	78.032	First Flap-wise (blade)	81.369	First Flap-wise (blade)
3	78.045	First Flap-wise (blade)	81.384	First Flap-wise (blade)
4	78.061	First Flap-wise (blade)	81.405	First Flap-wise (blade)
5	78.083	First Flap-wise (blade)	81.427	First Flap-wise (blade)
6	78.101	First Flap-wise (blade)	81.449	First Flap-wise (blade)
7	492.93	Second Flap-wise (blade)	283.36	First torsional (disk) + First flap-wise (blade)
8	493.04	Second Flap-wise (blade)	460.4	First Bending (shaft) + Second flap-wise (blade)
9	493.09	Second Flap-wise (blade)	461.5	First Bending (shaft) + Second flap-wise (blade)
10	493.4	Second Flap-wise (blade)	481.65	First Bending (shaft) + Third flap-wise (blade)
11	493.53	Second Flap-wise (blade)	482.58	First Bending (shaft) + Third flap-wise (blade)
12	493.9	Second Flap-wise (blade)	507.74	Forth Flap-wise (blade)
13	572.21	First Edgewise (blade)	507.94	Forth Flap-wise (blade)
14	573.46	First Edgewise (blade)	508.79	Forth Flap-wise (blade)
15	578.61	First Edgewise (blade)	508.83	Forth Flap-wise (blade)
16	581.01	First Edgewise (blade)	519.12	Fifth Flap-wise (blade)
17	582.91	First Edgewise (blade)	519.41	Fifth Flap-wise (blade)
18	596.7	First Edgewise (blade)	545.38	First Edgewise (blade)
19	764.84	First torsional (blade)	546.17	Frist Edgewise (blade)

Table 3. Pre-stressed Modal Analysis

Mode	Natural Frequency of Rotor (Hz)			Vibrational Mode
	Pre-stressed Modal Analysis			
	1000rpm	1500rpm	2000rpm	
1	86.562	94.741	104.74	First Flap-wise (blade)
2	86.816	95.071	105.19	First Flap-wise (blade)
3	86.937	95.189	105.31	First Flap-wise (blade)
4	87.038	95.298	105.43	First Flap-wise (blade)
5	87.078	95.34	105.47	First Flap-wise (blade)
6	87.343	95.603	105.73	First Flap-wise (blade)
7	277.42	277.81	278.33	First torsional (rotor) + First Flap wise (blade)
8	438.43	438.66	438.93	First Bending (shaft) + First Edgewise (blade) + Second Flap-wise (blade)
9	440.06	440.30	440.56	First Shaft Bending + First Edgewise + Second Flap-wise
10	467.66	469.35	471.17	First Shaft Bending + Third Flap-wise
11	469.64	471.38	473.24	First Shaft Bending + Third Flap-wise
12	504.6	513.69	524.42	Third Flap-wise (blade)
13	504.71	514.86	527.78	Third Flap-wise (blade)
14	505.79	515.83	528.48	Third Flap-wise (blade)
15	506.8	517.05	531.17	Third Flap-wise (blade)
16	513.68	522.95	536.06	Forth Flap-wise (blade)
17	514.87	524.13	537.21	Forth Flap-wise (blade)
18	538.00	539.59	542.72	First Edgewise + First Flap-wise (blade)
19	538.29	539.94	543.28	First Edgewise + First Flap-wise (blade)

The mode shapes and natural frequencies of both unstressed and pre-stressed models are tabulated in Table 2) and Table 3) respectively, with the description for each mode shape of the structure at 1000rpm 1500rpm and 2000rpm.

3. Results and Discussions

3.1. Observations on Dynamic Behavior of rotor-stator model at 1000rpm

Figure *3*3(a), (b) and (c) showed a presence of smaller vibration excitation when the collision (rub) between stator blade and rotor blade occurred during the run-up process where t = 0 to 0.2 seconds. After t = 0.2 seconds, the displacement pattern changed where the rotor was whirling at a constant rotational speed of 1000rpm. The amplitude of the vibration is much higher compare to the vibration at run-up process. It was observed that the blade has undergone resonance in a flap-wise vibrational mode in the x-direction, bending vibration mode in the y-direction and edgewise vibrational mode in the z-direction. It is possible that the occurrence of resonance could lead to large deflection on the blade when the collision (rub) excite more vibration. The rubbing force in Figure 3 (d), when the collision between the rotor blade and stator blade occurred and when the 6 rotor blades with the stator blades. During the run-up process at t = 0 to 0.2 seconds, one of the six blades was experienced a higher level of rubbing level of 2548.5N and 3042.5N. The reason is that the stator blade was rubbing with rotor blade when the penetration depth was changed to a higher depth more than the initial penetration depth of 6mm due to the vibration of the blade. The rotor rubs against the stator would excite the vibration amplitude. The highest level of rubbing force was found to be 4128N during the run-down process.
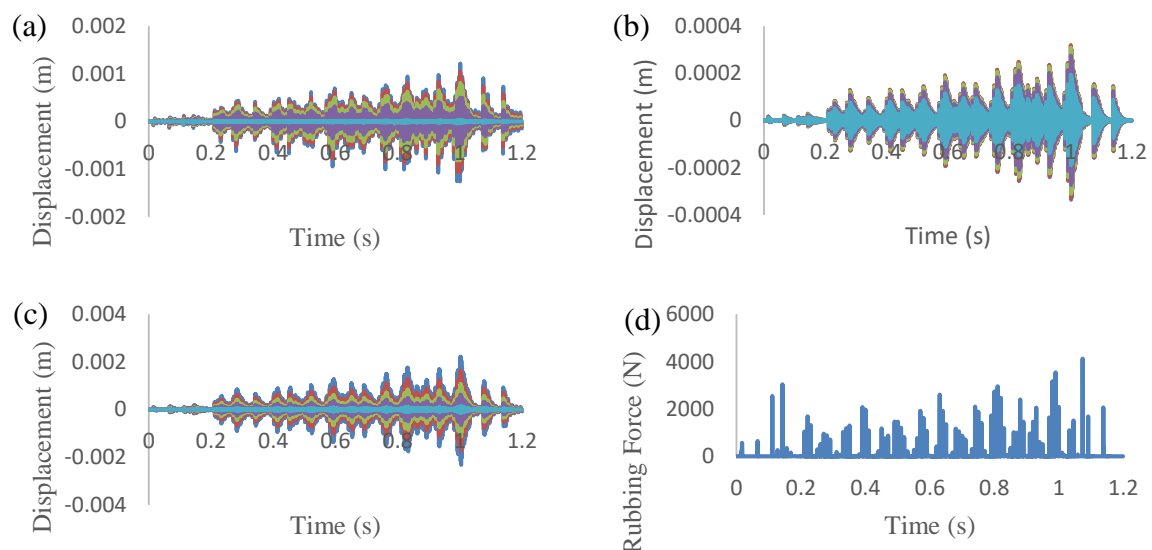

Figure 3. (a) Displacement of Stator Blade against Time (1000rpm, x-direction), (b) Displacement of Stator Blade against Time (1000rpm, y-direction), (c) Displacement of Stator Blade against Time (1000rpm, z-direction), (d) Rubbing Force at 1000rpm

3.2. Observations on Dynamic Behavior of rotor-stator model at 1500rpm

At running speed of 1500 rpm, during the run-up process, the stator blade has undergoes to a steady-state vibration when the rubbing between the stator blade and 6 rotor blades occurred. There is no presence of higher amplitude of excited vibrations showed to coincide with any of the natural frequencies as shown in Figure 4(a), (b) and (c). The pattern of the vibration has changed after t = 0.2 seconds and the rotor was whiling at a constant rotational speed of 1500rpm. It was observed that the vibration's features of the stator blade were identical with the vibration's features of the stator blades at

the rotational speed of 1500rpm. During the run-down process (t= 1.0 to 1.2 seconds) the rotor vibration was gradually decreased the whirling speed, the excited vibration of the stator blade was gradually decreased and there was no any resonance occurred by coinciding with excitation resonant frequencies during rubbing. By comparing the features of vibrations in all directions, the stator blade at 1500rpm was experienced a higher vibration (displacement) than the stator blade at 1000rpm during axial rubbing condition. Therefore, it could be concluded that the vibration of the stator blade will become severe when the rotational speed increased. (Ma, Yin, et al 2016).Besides, less rubbing forces were recorded during the run-up process and the run-down process according to Figure 4(d). This proved that the penetration depth did not alter much compare to the initial penetration depth of 6mm and only the occurrence of higher rubbing levels at constant rotational speed. It was possible that the larger vibration of the blade was due to the occurrence of resonance at t = 0.2 seconds to t = 1 seconds and also caused the alteration of penetration depth between the stator blade and rotor blade where a stator blade was rub with six rotor blade during whirling motion of the rotor. During rotational speed of 1500rpm, some of the blades were experienced the intermittent rubs but some did not due to the changed of penetration depth.
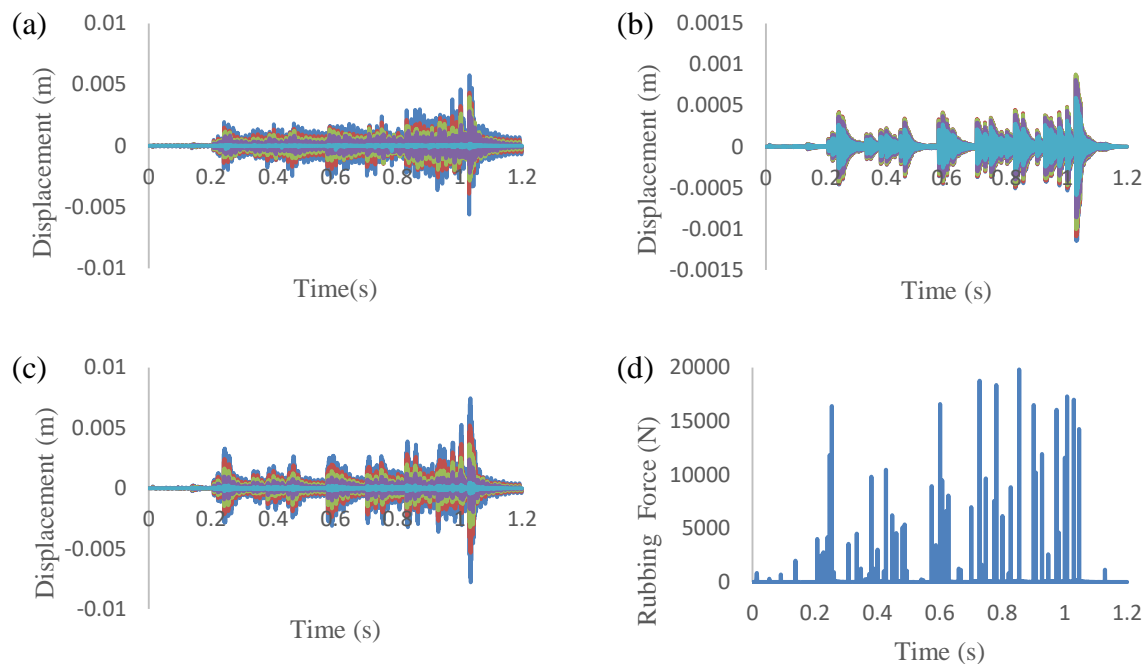

Figure 4. (a) Displacement of Stator Blade against Time (1500rpm, x-direction), (b) Displacement of Stator Blade against Time (1500rpm, y-direction), (c) Displacement of Stator Blade against Time (1500rpm, z-direction), (d) Rubbing Force under 1500rpm

3.3. Frequency Response of vibration at 1000rpm
The frequency response of the rotor system is obtained by Fast Fourier Transform (FFT) analysis to study the characteristic behaviour of the rotor system when rubbing event occurred in the rotor system. Figure 55(a) shows the healthy data of the measured vibration of the blade where no rubbing events. The fluctuation of the complicated non-linear frequency was not occurred due to no rubs events and there was only the appearance of the rotating speed frequency (16.67Hz) and its multiple frequencies

(6fr = 100Hz) which are also known as the blade passing frequency (BPF = 100). The blade passing frequency only occurs in real condition for healthy data of the rotor-stator model. Based on Figure *5*5(b), (c) and (d), which shows the frequency response of the rotor system at x, y and z directions. Figure 5(b, c and d) presenting the axial rubbing conditions at x, y and z-direction, respectively. That the appearance of the amplitudes of blade passing frequency (6fr, BPF) and its multiple frequency in x, y and z-direction such as BPF, 2BPF, 3BPF, 4BPF, 5BPF, 6BPF, 7BPF, 8BPF, 9BPF, 10BPF and 11BPF, i.e., 6fr, 12fr, 18fr, 24fr, 30fr, 36fr, 42fr, 48fr, 54fr, 60fr and 66fr. The vibration of the blade was excited due to the intermittent rubs. One of the multiple frequency (30fr, 5BPF) in x, y and z-direction was coincided with the Third flap-wise natural frequency of the rotor blade at 1000rpm based on the pre-stressed modal analysis in Table 3 where the natural frequency of 504.6Hz in mode 12 is nearly near to the blade passing frequency (30fr, 5BPF). The coincidence between natural frequency of rotor blade and blade passing frequency was showed to be more significant in the z-direction (axial rubbing condition) which was obtained the highest amplitude of 0.29mm. Meanwhile, the frequency of 77.5 Hz with the amplitudes of 54μm and 29.8μm appeared in x and z-direction respectively but it was observed that it did not coincide with any of natural frequency.
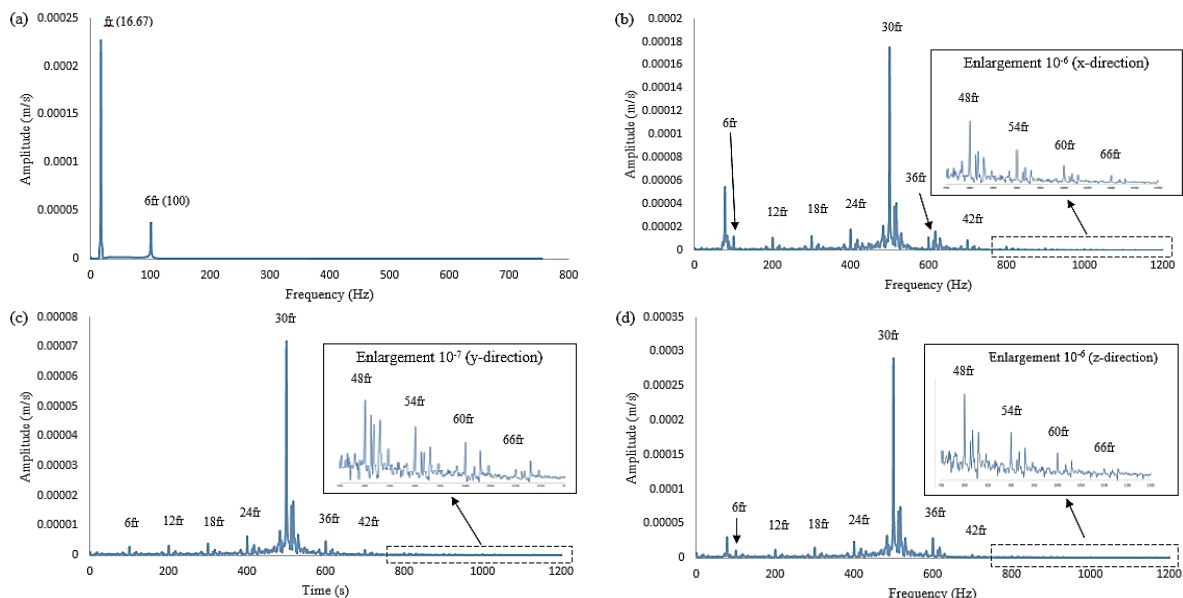

Figure 5. (a) Frequency Response at 1000rpm (Healthy Data), (b) Frequency Response at 1000rpm (x-direction), (c) Frequency Response at 1000rpm (y-direction), (d)Frequency Response at 1000rpm (z-direction).

3.4. Frequency Response of vibration at 1500rpm

Figure 6 illustrate the frequency response of the rotor system at 1500rpm with axial rub induced. Figure *6*6(b) and (d) shows that the appearance of the amplitudes of blade passing frequency (6fr, BPF) and its multiple frequencies in x, and z-direction such as BPF, 2BPF, 3BPF, 4BPF, 5BPF, 6BPF, 7BPF, 8BPF, 9BPF, 10BPF and 11BPF, i.e., 6fr, 12fr, 18fr, 24fr, 30fr, 36fr, 42fr and 48fr. One of the multiple frequencies (78Hz) was coincided with the First flap-wise natural frequency of the stator blade based on the unstressed modal analysis where the natural frequency of 78.016Hz is nearly near to the multiple frequencies (78Hz). Meanwhile, the frequency of 513 Hz with the amplitudes of 151μm but it was observed that it did not coincide with any of natural frequencies. Consequently, the coincidence was occurred between the one of the multiple frequencies (513Hz) and the natural frequency of rotor blade

at 1500rpm with high amplitude of 63.3μm in y direction in Figure *6*6(c) based on the pre-stressed modal analysis with the effect of centrifugal where the Third Flap-wise natural frequency of 513.69 Hz in mode 12 is nearly closed to the frequency of 513Hz. Subsequently, the severe resonance was occurred in the frequency response in the z-direction in Figure *6*6(d) due to the two high amplitudes of 169μm and 256μm under rubbing condition. The frequency of 78Hz and 513Hz were coincided with the First Flap wise and Forth Flap-wise natural frequency respectively based on the modal analysis in Table 2 and Table 3.
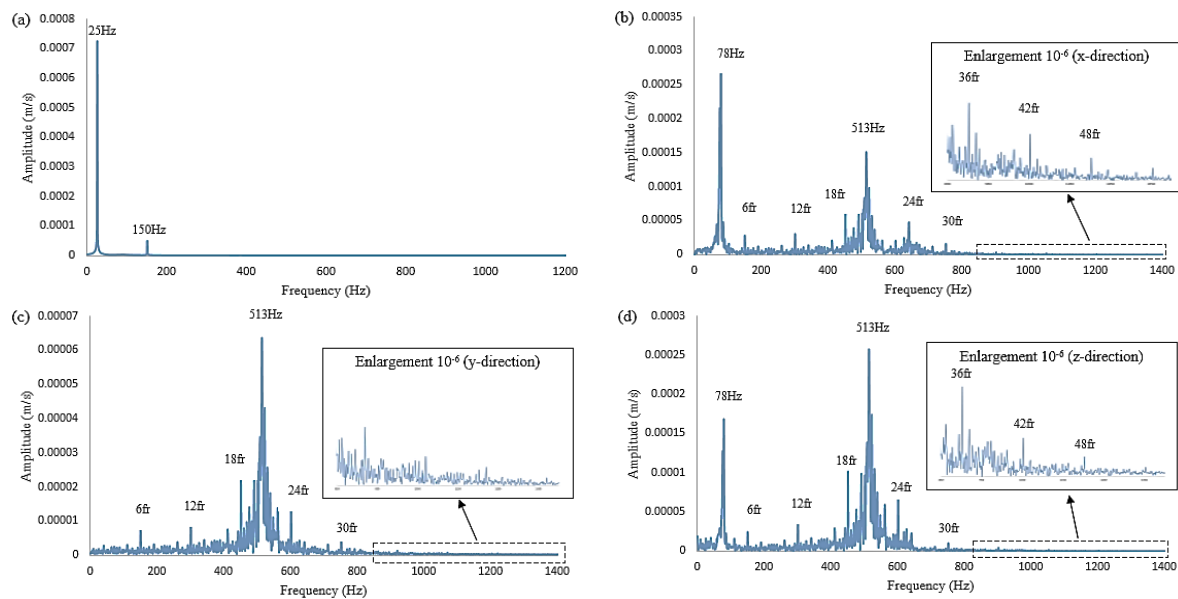

Figure 6. (a) Frequency Response at 1500rpm (Healthy Data), (b) Frequency Response at 1500rpm (x-direction), (c) Frequency Response at 1500rpm (y-direction), (d)Frequency Response at 1500rpm (z-direction).

3.5. Frequency Response of Vibration at 2000rpm

Figure *7*7 shows the frequency responses of the rotor system at a rotational speed of 2000rpm. It showed to be much complex compared to the frequency response at 1000rpm and 1500rpm. The blade passing frequency of 200Hz at 2000rpm and its multiple frequencies appeared and it was strongly proved that the amplitude of blade passing frequency of 200Hz was much higher due to the number of rotate cycles for the intermittent rubs between the stator blade and the six rotor blades.

Besides, the frequency of 84Hz with the amplitudes of 392μm and 155μm in x and z-direction respectively were coincided with the natural frequency of rotor blade where the frequency of 84Hz was nearly closed to the First Flap-wise natural frequency of 81 Hz according to the unstressed modal analysis in Table 2. Meanwhile, it was clearly that the frequency of 547Hz with the amplitudes of 52.5μm and 213μm in y and z-direction respectively were coincided with the natural frequency of rotor blade as the frequency of 547Hz was nearly closed to the First Edgewise natural frequency of 546.17 Hz at 2000rpm based on the unstressed modal analysis. Furthermore, the blade passing frequency in all direction at 2000rpm will be excited by increasing the rotational speed compared to the blade passing frequency at 1000rpm and 1500rpm.

Figure *7*7 also clearly illustrated that the occurrence of severe resonance due to the appearance of high amplitudes which is more than the resonance happened at the rotational speed of 1000rpm and

1500rpm. The more the number of rotate cycles, the more the interaction between the rotor blade and stator blade.
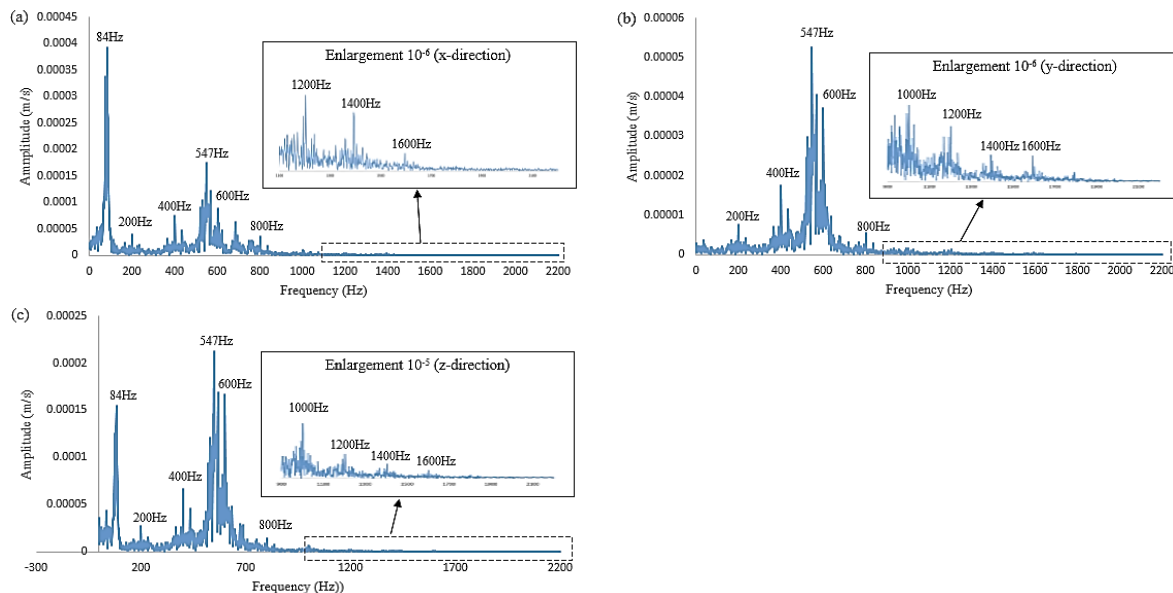

Figure 7. (a) Frequency Response at 2000rpm (x-direction), (c) Frequency Response at 2000rpm (y-direction), and (d) Frequency Response at 2000 rpm (z-direction)

3.6. Comparison between Axial and radial Rub Frequency's Response

Figure 8 shows the frequency response of the rotor system with radial blade rub induced fault at 1000rpm. It is clear that the blade passing frequency of 100Hz with the amplitude of 0.154μm and its multiple frequencies of 300Hz and 400Hz significantly appeared in y direction among x and z directions. This is possibly due to the fact that the occurrence of radial rub-impact between the tip of the rotor blade and inner casing happens in the y direction. Meanwhile, rotating frequencies of 16Hz, 40Hz and 31Hz with high amplitudes of 0.814μm, 2.96μm and 0.361μm respectively were coincided with the natural frequency of the casing due to the rotating frequencies during rubbing events were nearly closed to the natural frequency of casing based on the modal analysis of casing in Table 3. By comparing the frequency response of radial rub-impact in all direction figure (7) with the frequency response of axial rub-impact in (Figure 5̶5) at rotating speed of 1000rpm, the appearance of blade passing frequency of 100Hz with the amplitude of 0.00238μm and 0.154μm in x and y-direction respectively from the casing when the six rotor blade were contacted with the inner casing. But the blade passing frequency did not appear in the frequency response in the z direction. This is because the appearance of blade passing frequency was more significantly in y-direction when the tip of the rotor blade rub with casing in the y direction. However, it was observed that the amplitudes of blade passing frequencies for radial rub-impact were relatively smaller than amplitudes of the blade passing frequencies for axial rub-impact at the same operating speed and simulation conditions. This due to the effect of the casing which might cause less vibration. Some of the vibration caused by the rotor blade by collision (rub) might be neutralized by the overall of the casing that made up of steel material. Besides, by comparing the rubbing force in Figure 8 for radial rub-impact with axial rub-impact in Figure 5̶5(d), it was observed that the highest rubbing force occurred is only 4.75N only between the rotor blade and inner upper casing compared to the axial rub-impact. For the axial rub-impact, the highest rubbing force of 4128N is recorded between stator blade and rotor blade.
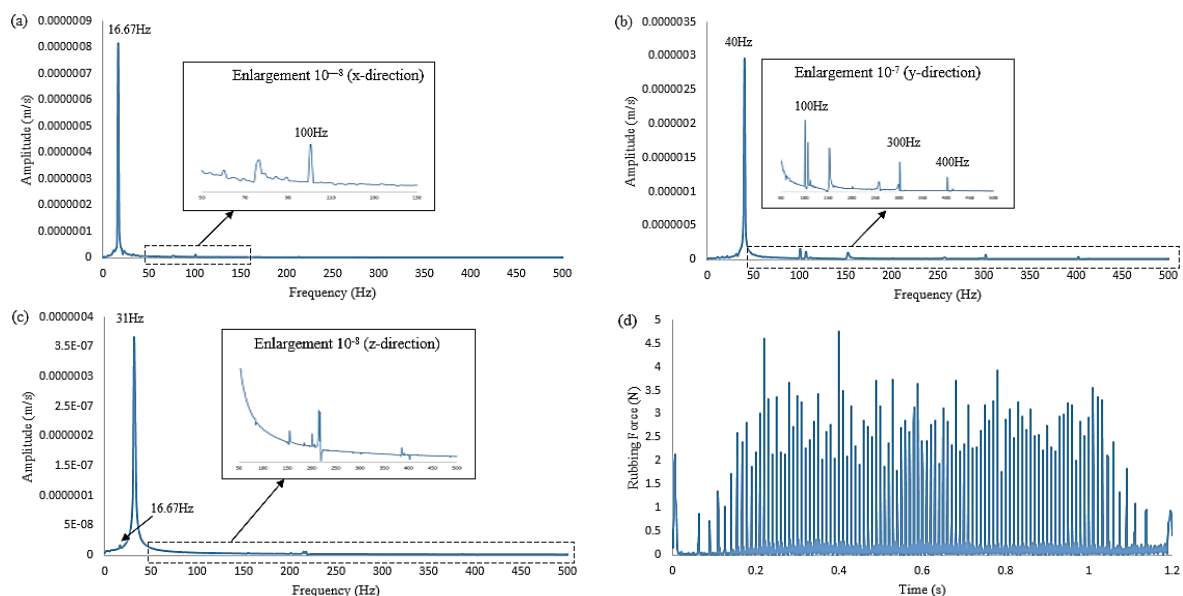
Figure 8. (a) Frequency Response at 1000rpm in Radial Rub Impact (x-direction), (b) Frequency Response at 1000rpm in Radial Rub Impact (y-direction), (c) Frequency Response at 1000rpm in Radial Rub Impact (z-direction), (d)Rubbing Force.

4. Conclusion

In this study, vibration response of axial and radial blade rubbing conditions in a rotor system were investigated using numerical simulation in ANSYS Software. The vibration response in all direction of axial rubbing was investigated at the rotational speed of 1000rpm, 1500rpm and 2000rpm. The rotor frequency response was obtained using Fast Fourier Transform (FFT) for the further investigation of the vibration's characteristics during the rubbing events. The blade passing frequency (BPF) and its multiple harmonic frequencies obviously appeared in x, y, and z-direction when the 6 rotor blades were rubbing with a stator blade 1 in the axial direction at the rotational speed of 1000rpm, 1500rpm and 2000rpm. With increasing the intermittent rubs by increasing the rotational speed, the blade passing frequency would be excited and also increased with high amplitudes. By comparing the frequency response at 1000rpm and 1500rpm with 2000rpm for blade axial rub it could be concluded that the more severe resonances with high amplitudes occurred at the higher rotational speed (2000rpm). Furthermore, it was clear that there was a difference between the axial rub-impact and radial rub-impact. The rub between blade to blade in the axial direction is showed to be more severe than the rub between the blade tips to the inner surface of the casing after the vibration response of the rotor-stator model and rotor-casing model was investigated and compared. The rubbing forces generated due to the blades axial rubs and blades radial rubs was also investigated and evaluated in this study and it was found that the blades axial rubs would generate a higher rubbing force than blades axial rubs, which may lead to fast machine failure compared to radial blade rubbing.

References

[1]   Abdelrhman A M, Hee L M, Leong M and Al-Obaidi S. 2014. Condition Monitoring of Blade in Turbomachinery: A Review. *Advances in Mechanical Engineering*.**6**. 210717

[2]   Abdelrhman A M, Leong M S, Saeed S A M and Al Obiadi S M. 2012 A review of vibration monitoring as a diagnostic tool for turbine blade faults. In: *Applied Mechanics and Materials,* Trans Tech Publ). pp. 1459-63

[3]   Zhang H and Chen Y. 2011. Bifurcation analysis on full annular rub of a nonlinear rotor system. *Science China Technological Sciences*.**54**. 1977-85

[4]   Lu W and Chu F. 2014. Radial and torsional vibration characteristics of a rub rotor. *Nonlinear Dynamics*.**76**. 529-49

[5]   Tai X, Ma H, Liu F, Liu Y and Wen B. 2015. Stability and steady-state response analysis of a single rub-impact rotor system. *Archive of Applied Mechanics*.**85**. 133-48

[6]   Choy F and Padovan J. 1987. Non-linear transient analysis of rotor-casing rub events. *Journal of Sound and Vibration*.**113**. 529-45

[7]   Laverty W. 1982. Rub energetics of compressor blade tip seals. *Wear*.**75**. 1-20

[8]   Cao D, Yang Y, Chen H, Wang D, Jiang G, Li C, Wei J and Zhao K. 2016. A novel contact force model for the impact analysis of structures with coating and its experimental verification. *Mechanical Systems and Signal Processing*.**70**. 1056-72

[9]   Yuan Z, Chu F and Hao R. 2007. Simulation of rotor's axial rub-impact in full degrees of freedom. *Mechanism and Machine Theory*.**42**. 763-75

[10]   Zhang K and Ding Q. 2009. Lateral and torsional vibrations of a two-disk rotor-stator system with axial contact/rubs. *International Journal of Applied Mechanics*.**1**. 305-26

[11]   Ma H, Yin F, Tai X, Wang D and Wen B. 2016. Vibration response analysis caused by rubbing between rotating blade and casing. *Journal of mechanical science and technology*.**30**. 1983-95

[12]   Ma H, Yin F, Wu Z, Tai X and Wen B. 2016. Nonlinear vibration response analysis of a rotor-blade system with blade-tip rubbing. *Nonlinear Dynamics*.**84**. 1225-58

[13]   Abdelrhman A M, Leong M S, Hee L M and Ngui W K. 2013 Application of wavelet analysis in blade faults diagnosis for multi-stages rotor system. In: *Applied Mechanics and Materials,* Trans Tech Publ). pp. 959-64

[14]   Abdelrhman A M, Leong M S, Hamdan Y M and Hui K H. 2015 Time Frequency Analysis for Blade Rub Detection in Multi Stage Rotor System. In: *Applied Mechanics and Materials,* Trans Tech Publ). pp. 95-9

[15]   Abdelrhman A M, Leong M S, Hee L M and Hui K H. 2014 Vibration analysis of multi stages rotor for blade faults diagnosis. In: *Advanced Materials Research,* Trans Tech Publ). pp. 133-7